Radio Science, Volume 36, Number 1, Pages 97–106, January–February 2001

Specification of channel filters for an interferometric radiometer

J. Bará, A. Camps, I. Corbella, and F. Torres
Polytechnic University of Catalonia, Barcelona, Spain

Abstract. Differences among the channels that form an interferometric radiometer result in amplitude and phase errors in the cross correlations measured from the signals collected by each pair of antennas (visibility samples). Since point source calibration of a satellite-embarked instrument operating in a radio astronomy protected band is, in principle, not possible, and although separable phase errors can be corrected, the nonseparable ones produce an irrecoverable loss of information and have to be kept below specified limits. Preliminary work performed by the authors established basic requirements on the channel transfer function so as to meet these strict specifications imposed by proper calibration and inversion procedures. These requirements were set, from a simple filter model, in terms of three basic parameters: center frequency, bandwidth, and overall group delay. The purpose of this work is, for any kind of filter, to translate these requirements into a given insertion loss mask that must be satisfied by all filters so as to keep nonseparable error terms under certain specified bounds. The numerical results and computer simulations presented are based on the specifications of MIRAS, a two-dimensional aperture synthesis radiometer currently under study by the European Space Agency, and its proposed in-orbit calibration procedure.

1. Introduction

The basic measurement of an interferometric radiometer is the so-called visibility function V_{12}, units of Kelvin, given by the cross correlation of the analytic voltage signals $b_1(t)$ and $b_2(t)$ collected by two antennas 1 and 2, located over the XY plane and spaced a normalized distance $(u_{12},v_{12}) = (x_2 - x_1, y_2 - y_1)/\lambda_0$ (λ_0 is the wavelength at the nominal center frequency), which is called the baseline [*Torres et al.*, 1997]:

$$V(u_{12},v_{12}) = \frac{1/2}{k_B\sqrt{B_1 B_2}\sqrt{G_1 G_2}} \frac{\langle b_1(t)\, b_2^*(t)\rangle}{\sqrt{\Omega_1\Omega_2}}$$

$$= \iint_{\xi^2+\eta^2\le 1} \frac{T_B(\xi,\eta)}{\sqrt{1-\xi^2-\eta^2}} F_{n1}(\xi,\eta)\, F_{n2}^*(\xi,\eta)$$

$$\cdot \tilde{r}_{12}\left(\frac{u_{12}\xi + v_{12}\eta}{f_0}\right) \exp[j2\pi(u_{12}\xi + v_{12}\eta)]\, d\xi\, d\eta, \quad (1)$$

where k_B is the Boltzmann constant, $B_{1,2}$ and $G_{1,2}$ are the noise bandwidth and the power gain of the receiving chains, respectively, $T_B(\xi, \eta)$ is the brightness temperature of the scene, $\Omega_{1,2}$ and $F_{n1,2}(\xi, \eta)$ are the equivalent solid angle and the normalized radiation voltage patterns of the antennas, respectively, $(\xi, \eta) = (\sin\theta\cos\phi, \sin\theta\sin\phi)$ are the director cosines with respect to the X and Y axes, respectively, and $\tilde{r}$ is the so-called fringe-washing function, which accounts for spatial decorrelation effects and depends on the normalized channels' frequency response, $H_{n1,2}(f)$, through [*Thomson et al.*, 1986; *Torres et al.*, 1997]

$$\tilde{r}_{12}(\tau) = \frac{e^{-j2\pi f_0\tau}}{\sqrt{B_1 B_2}} \int_0^\infty H_{n1}(f) H_{n2}^*(f) e^{j2\pi f\tau} df$$

$$= \frac{1}{\sqrt{B_1 B_2}} \mathrm{F}^{-1}\left[H_{n1}(f+f_0) H_{n2}^*(f+f_0) u(f+f_0)\right]. \quad (2)$$

2. Basic Properties of a Channel

It will be assumed that a "channel," that is, the electronic circuits between the antenna output and the input of an ideal, error-free complex correlator (Figure 1), is ideally formed by transmission lines or waveguides, or even optical fibers, amplifiers, down-converters, and narrowband band-pass filters such that (1) the transmission lines, etc., are accurately described,

Paper number 1998RS002140.
0048-6604/01/1998RS002140$11.00

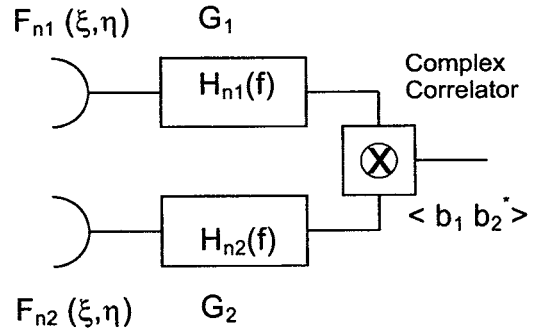

Figure 1. Scheme of two receiving channels and a complex correlator forming a baseline.

within the band, by constant attenuation and a phase linear with frequency (constant group delay), (2) the amplifiers and down-converters are also assumed to have a flat response within the band so that assumption 1 applies, and (3), as pointed out above, the nonidealities introduced by the correlator are not accounted for.

Consequently, provided the filter is narrowband so that the low-pass to band-pass transformation used in the filter design can be approximated by a linear shift to the band center frequency f_0,

$$f' = \frac{f}{f_0} - \frac{f_0}{f} \approx 2\,\frac{f - f_0}{f_0}, \quad |f - f_0| << f_0; \tag{3}$$

the frequency response of the the kth channel can be expressed as

$$H_k(f) = \sqrt{G_k} H_{nk}(f)$$
$$\sqrt{G_k}\exp[j\phi_k - j2\pi(f - f_0)\tau_k] H_{ok}(f - f_o) \quad f > f_o,$$
$$H_k(f) = 0 \qquad f < f_o, \tag{4}$$

where ϕ_k and τ_k are the constant phase and group delay as explained in assumptions 1 and 2 above, $H_{ok}(f)$ is the normalized (max $H_{ok}(f)$ = 1) low-pass prototype frequency response, and $H_{nk}(f)$ is the normalized channel frequency response. Written in this form, and assuming negligible losses in the filter itself, $H_{ok}(f)$ is known to be an analytic signal in the frequency domain; that is, its Fourier transform vanishes for negative time values. (This is not to be confused with analytic function in a given domain in the strict mathematical sense. Note also that shifting a function in the vertical direction in the complex frequency plane, $s = \sigma + jw$, does not change its analytic signal character, linked to the values of the real parts of its poles and zeroes.) This function can also be expressed in terms of the ideal filter transfer function $H_o(f)$ as:

$$H_{ok}(f) = H_o(f) D_k(f), \tag{5}$$

where $D_k(f)$ is a deviation function that can be interpreted as another filter cascaded with the ideal one (Figure 2).

For the most common kinds of pass-band filters (Butterworth, all-pole Tchebycheff, inverse Tchebycheff, and Cauer) the transfer function will either have no zeroes or have them lying in the imaginary axis. In these cases, D_k will be also an analytic signal in the frequency domain. If $D_k(f)$ is written as

$$D_k(f) = \exp[-A_k(f) + j\Phi_k(f)], \tag{6}$$

with $A_k(f)$ and $\Phi_k(f)$ being real signals, then, if $A_k(\infty) = 0$, the deviation phase $\Phi_k(f)$ is the Hilbert transform of the deviation attenuation $A_k(f)$ [*Van Valkenburg*, 1955]:

$$A_k(f) = -\Phi_k(f) * \frac{1}{\pi f} \quad \Leftrightarrow \quad \Phi_k(f) = A_k(f) * \frac{1}{\pi f}, \tag{7}$$

where the star stands for convolution operator. The notation can be shortened by defining

$$\mathbf{A}_k(f) = A_k(f) + j\Phi_k(f) \;\Rightarrow\; D_k(f) = \exp[-\mathbf{A}_k^*(f)]. \tag{8}$$

Some properties of $A_k(f)$ that are used in later developments are provided in appendix A.

3. Fringe-Washing Function and Phase Separability

The interest is focused in the computation of the fringe-washing (or decorrelation) function associated with two channels as given by (2). Let us write it again as

$$\tilde{r}_{12}(\tau) = \exp[j(\phi_1 - \phi_2)]\frac{S_{12}(\tau - \tau_1 + \tau_2)}{\sqrt{B_1 B_2}}, \tag{9}$$

$$S_{12}(\tau) \triangleq \int_{-\infty}^{\infty} H_{o1}(f) H_{o2}^* e^{j2\pi f\tau}\, df \quad B_i = S_{ii}(0) \tag{10}$$

(the delta over equals symbol stands for equal by definition). In the first place, it can be seen that the phase information of the fringe-washing function resides in S_{12}, apart from the ϕ_1 - ϕ_2 term (phases contributed by amplifiers, transmission media, and down-converters). Substituting (5) into (10),

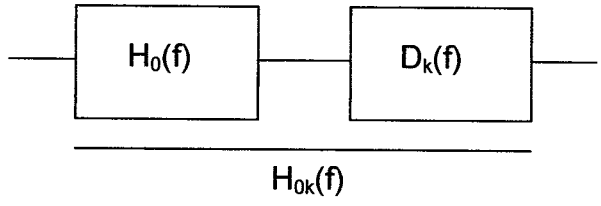

Figure 2. Representation of a nonideal filter as an ideal filter cascaded with a deviation filter.

$$S_{12}(\tau) = \int_{-\infty}^{\infty} |H_o(f)|^2 D_1(f) D_2^*(f) e^{j2\pi f\tau}\, df$$

$$= \int_{-\infty}^{\infty} T(f) \exp[-(\mathbf{A}_1^* + \mathbf{A}_2)] e^{j2\pi f\tau}\, df, \qquad (11)$$

with $T(f) \quad |H_o(f)|^2$. Note first that $T(f)$ is a symmetric function, and in the case of ideal filters, ($D_1 = D_2 = 1$) $S_{12} = S(\tau)$ will be real. Furthermore, for an ideal high-order filter (n > 5) $S(\tau)$ will be very close to a sinc function:

$$S(\tau) \approx B\,\mathrm{sinc}(B\tau). \qquad (12)$$

Second, the delays τ_1 and τ_2 in (9) can be very accurately controlled: to ~0.04 ns for 1 cm length error in the transmission lines (solid Teflon coaxial cable) and to ~1 ns for the amplifier and down-converter contribution. It will be then assumed that these delays are adjusted so that their net contribution to (9) is negligible (this point leads, anyway, to a complex process whose analysis is beyond the paper scope: The reader may refer to *Camps et al.* [1999] for a discussion of baseline fringe-washing function characterization).

Because of the characteristics of the calibration procedures [*Torres et al.*, 1996; *Martín-Neira and Goutoule*, 1997] it is important to split the phase of the fringe-washing function into its separable and non separable parts:

$$\tilde{r}_{12}(\tau) = |\tilde{r}_{12}(\tau)| \exp\,[j(\psi_1 + \psi_2 + \psi_{12}^{ns})]\,, \qquad (13)$$

where ψ_1 and ψ_2 (separable terms) are contributed by channels 1 and 2 independently. If the nonseparable term ψ_{12}^{ns} vanishes for all possible baselines, the phase information of the fringe-washing functions can be recovered from the phase closure property of a set of baselines that form a closed contour [*Torres et al.*, 1997], or by distributed noise injection calibration techniques [*Torres et al.*, 1996].

From (9) and (13) it is clear that ϕ_1 and ϕ_2 are separable. To investigate the phase separability of S_{12}, the exponential within the integral in (11) can be expanded in a Taylor series, and by grouping those terms comprising only $\mathbf{A}_1$ or $\mathbf{A}_2$ and those comprising products of these functions, we obtain

$$e^{-(\mathbf{A}_1^* + \mathbf{A}_2)} = 1 - (\mathbf{A}_1^* + \mathbf{A}_2) + \frac{1}{2}(\mathbf{A}_1^* + \mathbf{A}_2)^2 + \cdots$$

$$= 1 + [\exp(-\mathbf{A}_1^*) - 1] + [\exp(-\mathbf{A}_2) - 1] + \mathbf{A}_1^*\,\mathbf{A}_2$$

$$+ F(\mathbf{A}_1^{*m}\,\mathbf{A}_2^n) \quad m+n \geq 3, \qquad (14)$$

from which S_{12} can be decomposed into its separable and nonseparable parts:

$$S_{12}(\tau) = S(\tau) + \Delta S_1(\tau) + \Delta S_2(\tau) + \Delta S_{12}^{(2)}(\tau) + \Delta S_{12}^{(>3)}(\tau)$$

$$S(\tau) = \mathrm{F}^{-1}[T(f)], \quad \Delta S_1(\tau) = \mathrm{F}^{-1}\left(T(f)[\exp(-\mathbf{A}_1^*) - 1]\right),$$

$$\Delta S_2(\tau) = \mathrm{F}^{-1}\left(T(f)[\exp(-\mathbf{A}_2) - 1]\right),$$

$$\Delta S_{12}^{ns}(\tau) = \Delta S_{12}^{(2)}(\tau) + \Delta S_{12}^{(>3)}(\tau) = \mathrm{F}^{-1}[T(f)\mathbf{A}_1^*\mathbf{A}_2]$$

$$+ \mathrm{F}^{-1}[T(f)F(\mathbf{A}_1^{*m}\mathbf{A}_2^n)], \quad m+n \geq 3. \qquad (15)$$

The notation emphasizes the fact that, while ΔS_i are terms of first order on A_i, the nonseparable part ΔS_{12}^{ns} has terms of second order and higher. The next step is the evaluation of the phase of S_{12}. It is shown in appendix B that if

$$|S(\tau)| \geq |\Delta S_1(\tau)| + |\Delta S_2(\tau)| + |\Delta S_{12}^{(2)}(\tau)| + |\Delta S_{12}^{(>3)}(\tau)|, \qquad (16)$$

then:

$$\psi_1(\tau) = \arg\left[S(\tau) + \Delta S_1(\tau)\right] = \arg \int_{-\infty}^{\infty} T(f) \exp[-\mathbf{A}_1^*] e^{j2\pi f\tau} df,$$

$$\psi_2(\tau) = \arg \int_{-\infty}^{\infty} T(f) \exp[-\mathbf{A}_2] e^{j2\pi f\tau} df$$

$$\psi_{12}^{ns}(\tau) \approx -\,\mathrm{Im}\left(\frac{\Delta S_1(\tau)}{S(\tau)} \frac{\Delta S_2(\tau)}{S(\tau)}\right) + \arg\left[S(\tau) + \Delta S_{12}^{(2)}(\tau)\right], \qquad (17)$$

where only terms of first and second order have been retained. It can be seen that the nonseparable phase error is a second-order effect.

4. First- and Second-Order Approximations

When the attenuation deviations are small enough to neglect second-order terms, we have

$$\Delta S_{12}(\tau) \quad \Delta S_1(\tau) + \Delta S_2(\tau)$$

$$\approx -\int_{-\infty}^{\infty} T(f)[\mathbf{A}_1^*(f) + \mathbf{A}_2(f)]\, e^{j2\pi f\tau} df. \qquad (18)$$

Note that since $e^x \approx 1 + x + x^2/2! + x^3/3! + \cdots$, if an error of a few units percent, say 5%, can be accepted, the approximations implicit in (18) are valid for deviation attenuations A_k up to 0.32 Np = 2.78 dB.

It is shown (appendix C) that for high-order filters ($n \geq 5$) and a given upper bound of the deviation attenuation σ_A, defined by

$$\int_{-f_M}^{f_M} |A_k(f)|^2 df \leq B_M \sigma_A^2 \quad (f_M = 1.3 f_c;\ B_M = 2 f_M), \qquad (19)$$

where f_c is the ideal filter prototype cutoff frequency, then

$$|\Delta S_{12}(\tau)| \leq 2.2 \sqrt{\alpha}\, B \sigma_A, \qquad (20)$$

with α being a constant close to unity, unknown so far, but such that if f_M becomes large, then α tends to 1.

4.1. Phase Errors

For angles small enough to neglect second-order terms, the separable phase term (first order in ΔS) can be approximated by

$$\psi_{12}^{s} \quad \psi_1(0)+\psi_2(0) \approx \frac{\Delta S_1^i}{S+\Delta S_1^r}+\frac{\Delta S_2^i}{S+\Delta S_2^r}$$

$$= \frac{\Delta S_1^i (S-\Delta S_2^r)}{S^2-(\Delta S_1^r)^2}+\frac{\Delta S_2^i (S-\Delta S_1^r)}{S^2-(\Delta S_2^r)^2} \approx$$

$$\approx \frac{\Delta S_{12}^i}{S} \approx \frac{1}{B}\int_{-f_M}^{f_M} T(f)[\Phi_1(f)-\Phi_2(f)]df. \qquad (21)$$

Therefore

$$|\psi_{12}^{s}| \le \frac{|\Delta S_{12}|}{S} \le 2.2\ \sqrt{\alpha}\ \sigma_{A\ \mathrm{Np}}\ \mathrm{rad} = 4.5\ \sqrt{\alpha}\ \sigma_{A\ \mathrm{dB}}\ \mathrm{deg}, \qquad (22)$$

where we have introduced the units of each magnitude (radians or degrees, nepers or decibels). For the nonseparable terms, (17) can be rewritten as

$$\psi_{12}^{ns}(0) \approx -\mathrm{Im}\left(\frac{\Delta S_1 \Delta S_2}{S^2}\right)+\frac{\mathrm{Im}\left(\Delta S_{12}^{(2)}\right)}{S} \quad \psi_{12}^{ns'}+\psi_{12}^{ns''}. \qquad (23)$$

The terms $\psi_{12}^{ns'}$ and $\psi_{12}^{ns''}$ can be bound as follows (appendix C):

$$\left|\psi_{12}^{ns'}\right| \le \frac{|\Delta S_1 \Delta S_2|}{S^2} \approx \frac{1}{B^2}\left|\int_{-f_M}^{f_M} T(f)\mathbf{A}_1^{*}df\right|\left|\int_{-f_M}^{f_M} T(f)\mathbf{A}_2 df\right|$$

$$\le 4\frac{B'B_M}{B^2}\ \alpha\sigma_A^2 \approx 4.8\,\alpha\,\sigma_{A\ \mathrm{Np}}^2\ \mathrm{rad} = 3.6\,\alpha\,\sigma_{A\ \mathrm{dB}}^2\ \mathrm{deg}, \qquad (24a)$$

$$\left|\psi_{12}^{ns''}\right| = \frac{1}{B}\left|\mathrm{Im}\int_{-f_M}^{f_M} T(f)\mathbf{A}_1^{*}\mathbf{A}_2\,df\right| \le \frac{1}{B}\int_{-f_M}^{f_M} T(f)\,|\mathbf{A}_1^{*}\mathbf{A}_2|\,df$$

$$< \frac{1}{B}\int_{-f_M}^{f_M} \left|\mathbf{A}_1^{*}\mathbf{A}_2\right| df \le \frac{B_M}{B}\,4\alpha\sigma_A^2 \approx 5.2\,\alpha\sigma_A^2$$

$$= 3.9\,\alpha\,\sigma_{A\ \mathrm{dB}}^2\ \mathrm{deg}. \qquad (24b)$$

(B' as defined by equation (D2)). At this point, in order to avoid unduly large bounds, it seems reasonable to take as overall bound the rms sum of both second-order bounds (equations (24a) and (24b)):

$$|\psi_{12}^{ns}| \le \sqrt{4.8^2+5.2^2}\ \alpha\,\sigma_{A\ \mathrm{Np}}^2\ \mathrm{rad} = 5.4\,\alpha\,\sigma_{A\ \mathrm{dB}}^2\ \mathrm{deg}. \qquad (25)$$

It has been shown by *Torres et al.* [1996] that with an in-orbit calibration procedure based in a distributed noise injection system the maximum allowed nonseparable phase error value in order to achieve a radiometric resolution compatible with MIRAS objectives is 0.4° [*Torres et al.*, 1996; *Martín-Neira and Goutoule*, 1997]. From (25), it can be seen that, assuming $\alpha = 1$, a rms deviation attenuation bound of $\sigma_A = 0.27$ dB will result in a nonseparable phase error value below the required 0.4°. Under the same hypothesis the first-order phase variation is bounded by 3.9° (equation (22)).

4.2. Amplitude Errors

In the absence of errors the amplitude of the fringe-washing function at $\tau = 0$ takes the value 1 (equation (2)). It is shown in appendix 5 that:

$$\Delta|\tilde{r}_{12}| \approx -\frac{1}{B}\int_{-f_M}^{f_M} T(f)\,|\mathbf{A}_1^{*}(f)-\mathbf{A}_2(f)|^2 df$$

$$+\frac{1}{2B^2}\mathrm{Re}\left(\int_{-f_M}^{f_M} T(f)[\mathbf{A}_1^{*}(f)-\mathbf{A}_2(f)]df\right)^2, \qquad (26)$$

$$|\Delta|\tilde{r}_{12}|| < \frac{1}{B}\int_{-f_M}^{f_M} |\mathbf{A}_1^{*}(f)-\mathbf{A}_2(f)|^2 df$$

$$+\frac{1}{2B^2}\left|\int_{-f_M}^{f_M} T[\mathbf{A}_1^{*}(f)-\mathbf{A}_2(f)]df\right|^2$$

$$\le 16\alpha\frac{B_M}{B}\sigma_A^2+4\alpha\frac{B'B_M}{B^2}\sigma_A^2. \qquad (27)$$

It can be seen that amplitude errors are of second order and, by expansion of (26), that the separable and nonseparable parts are of the same order of magnitude, which invalidates a priori any amplitude restoration

Table 1. Summary of Theoretical Bounds for Phase/Amplitude Error Terms

Magnitude	Bound	Target	σ_A ($\alpha = 1$)
Separable phase error	$\lvert\psi_{12}^{s}\rvert \le 14.5\sqrt{\alpha}\,\sigma_{A\ \mathrm{dB}}$ deg	na	na
Nonseparable phase error	$\lvert\psi_{12}^{ns}\rvert < 5.4\,\alpha\,\sigma_{A\ \mathrm{dB}}^2$ deg	0.4 deg	0.27 dB
Amplitude error	$\lvert\Delta\lvert\tilde{r}_{12}\rvert\rvert < 0.28\,\alpha\,\sigma_{A\ \mathrm{dB}}^2$	0.003	0.10 dB

Here, na, not applicable.

algorithm. Note also that while the first term in (26) is always negative, the second one may be positive or negative. If we again compute the upper bound as the rms sum of both amplitude error terms in (27) rather than its direct sum, we obtain (with $B' = 0.92B$, $B_M = 1.3B$; refer to appendix D)

$$|\Delta|\tilde{r}_{12}||<21.4\alpha\sigma_A^2=0.28\,\alpha\,\sigma_{A\,\mathrm{dB}}^2. \qquad (28)$$

Again, with the in-orbit calibration procedure based in a distributed noise injection system mentioned in section 4.1[*Torres et al.*, 1996], the maximum-allowed amplitude error value in order to achieve the 1 K radiometric resolution objective in MIRAS requires an attenuation deviation σ_A of 0.10 dB or less: a stronger requirement than that of 0.27 dB for the phase as found in section 4.1. The theoretical bounds found so far are summarized in Table 1, as well as the corresponding values so as to make the calibration procedure compatible with the radiometric resolution target.

5. Numerical Simulations

Although the allowed attenuation deviations are adequately characterized through their norm or variance in the band $(-f_M, f_M) = (-1.3\,f_c,\ 1.3\,f_c)$, as explained in sections 4.1 and 4.2, from the point of view of the system designer it would be useful to have an attenuation mask (in an attenuation versus frequency plot, a region bounded by two lines between which the attenuation, or its deviation, has to lie) to accommodate all the individual filter deviation attenuation responses.

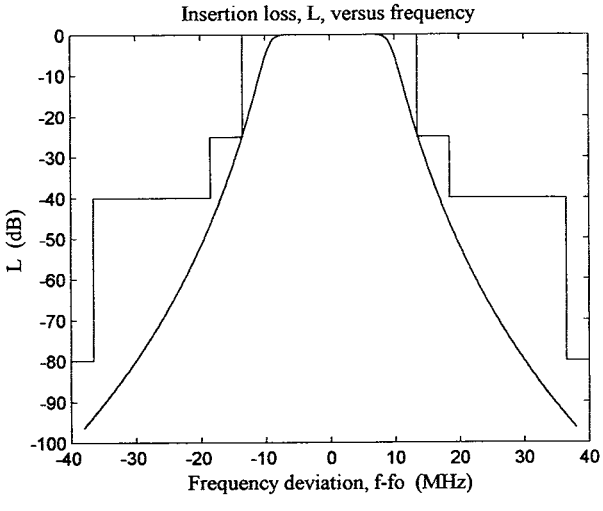

Figure 3. Filter mask as in conclusion 1 of section 5 and frequency response of an eighth-order Butterworth filter. It can be seen how the more strict mask requirement is imposed by the jump to 25 dB attenuation. Were it not for this, a seventh-order filter would meet the requirements.

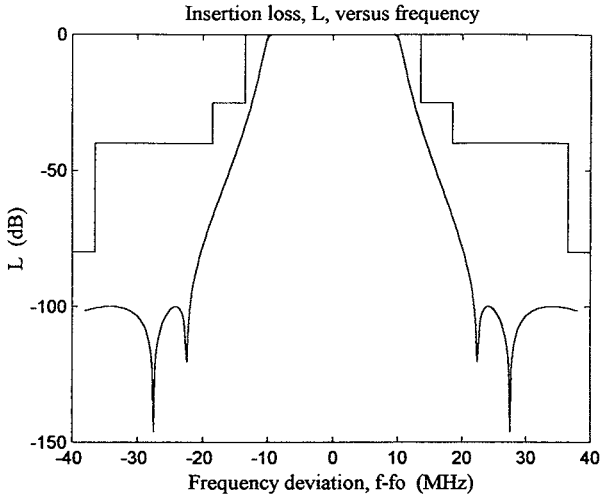

Figure 4. Frequency response of a seventh-order elliptic (Cauer) filter. Here $r_p = 0.043$ dB and $r_s = 100$ dB.

Also, the expressions found above are upper bounds that, as such, guarantee specification fulfillment, but the actual requirements may be less strict. To overcome those limitations, computer simulations have been performed in the following manner: (1) Filter specifications have been selected. Those used for MIRAS receiver development have been chosen. They require a 19 MHz bandwidth, >20 dB in-band return loss (< 0.0436 dB attenuation ripple), and an attenuation in the rejection band represented graphically in Figures 3 and 4 together with the theoretical response of different filter types. (2) A suitable filter prototype meeting the specifications (Butterworth, Tchebycheff, inverse Tchebycheff, and elliptic or Cauer) has been defined. (3) Errors have been introduced by means of normally distributed random shifts of the poles in the left complex plane and of the zeroes in the imaginary axis (these latter only for inverse Tchebycheff and Cauer filters). (4) For the filter with errors all the relevant phase and amplitude errors and the amplitude deviation rms value σ_{A12} in the range $(-1.3f_c, 1.3f_c)$ have been computed. At this point it is important to recall that the amplitude deviation $A_k(f)$ is defined so as to have zero average value in the quoted frequency interval (appendix A, paragraph 3). This is a weak form of the stronger, but experimentally difficult to test, underlying mathematical condition (equation A3)

$$\int_{-\infty}^{\infty} A_k(f)\,df = 0. \qquad (29)$$

Pole and zero relative error variances have been experimentally chosen so that in accordance with Table

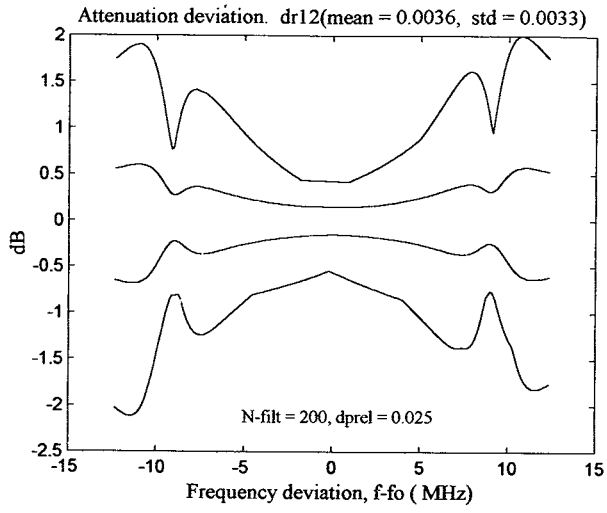

Figure 5. Attenuation deviation mask for an eigth-order Butterworth filter. Outer lines: all filters. Inner lines: 2/3 of the filters comprised. N-filt, number of filters used in the simulation; dprel, zero and pole random shifts variance.

1 the amplitude error standard value is approximately 0.03. Statistical variables are estimated from an ensemble of 200 filters. The following results were found.

1. The rms amplitude deviation attenuation $\sigma_{A1,2}$ is a random variable with mean close to 0.40 dB and standard deviation of 0.16 dB.

2. For separable phase errors, if we define the constant $C(\psi_1)$ such that for each filter,

$$\psi_k = C(\psi_k)\,\sigma_{Ak\,\mathrm{dB}}\ \mathrm{deg}, \tag{30}$$

it is found that ψ_1 is a zero-mean random variable with standard deviation between 1.5° and 3.5°, depending on the filter type, and $C(\psi_1)$ is also a zero mean random variable with stdandard deviation between 2.0 and 3.5. This value is compatible with the theoretical upper bound given in Table 1 if we assume it to be, approximately, 3 standard deviations and take $\alpha = 1$.

3. For nonseparable phase errors, let us define now the constant $C(\psi_{12}^{ns})$ such that for each filter,

$$\psi_{12}^{ns} = C(\psi_{12}^{ns})\,\sigma_{Ak\,\mathrm{dB}}\ \mathrm{deg}. \tag{31}$$

Again, ψ_{12}^{ns} is a zero-mean random variable with standard deviation near 0.1°, and $C(\psi_{12}^{ns})$ is also a zero-mean random variable with standard deviation between 0.45 and 0.65. This value is somewhat below the theoretical upper bound given in Table 1 under the 3 standard-deviations assumption.

4. For the amplitude error, defining again a constant $C(\Delta_{12})$ such that for each filter,

$$\Delta\tilde{r}_{12} = C(\Delta_{12})\,\sigma_{A\,\mathrm{dB}}, \tag{32}$$

now $\Delta\tilde{r}_{12}$ is a random variable with mean close to -0.003/-0.004 and standard deviation of approximately 0.0025/0.0035, while $C(\Delta_{12})$ has mean -0.03/-0.04 and standard deviation 0.035/0.045. As with the case of nonseparable phase error, these values are somewhat below the upper bound given in Table 1.

5. For the deviation attenuation mask, for each ensemble of 200 filters leading to the 0.003/0.004 amplitude error, a mask of the allowed filter deviation attenuation has been plotted in the following way (Figures 5 and 6): For each frequency the ensemble maximum and minimum values were first plotted (outer lines). Then, at each frequency the values corresponding to the standard deviations of the positive and negative attenuation deviation values have been also plotted (inner lines). In this way, the similarity requirement between different filters (channels) can be stated such that for all of them, their attenuation deviations are kept within the outer lines, and most of them are kept within the inner ones. (Probably two thirds of the filters should lie between the inner lines, although more precision cannot be given, since the probability distribution function is not known.)

Computer simulations have shown that these masks are critical; that is, small widenings tend to increase sharply the fringe-washing function amplitude error. Therefore a conservative mask should be adopted. Differences among the masks for different filter prototypes and changes in order by ±1 are difficult to

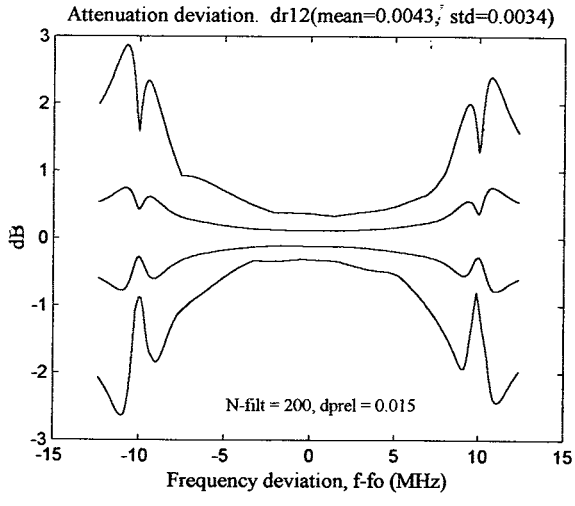

Figure 6. Attenuation deviation mask for filter shown in Figure 5. Outer lines: all filters. Inner lines: 2/3 of the filters comprised. The differences between this mask and those for other filters are difficult to discern, although the reduced zero and pole random shifts variance as compared to Butterworth (0.015 versus 0.032) indicate more critical filter repeatability.

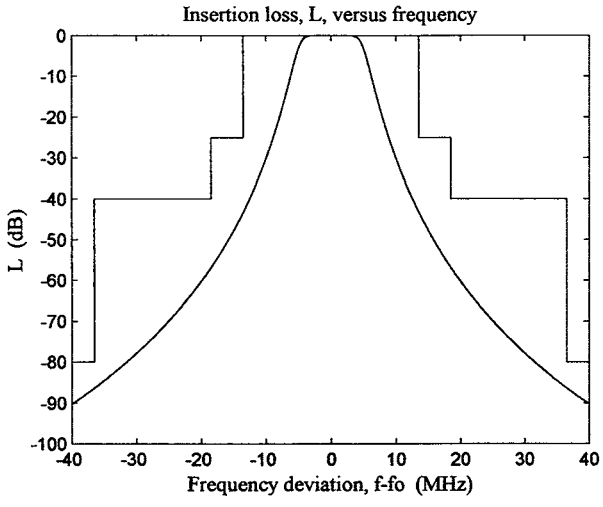

Figure 7. Filter mask as in conclusion 1 of section 5 and frequency response of a fifth-order, 10 MHz Butterworth filter.

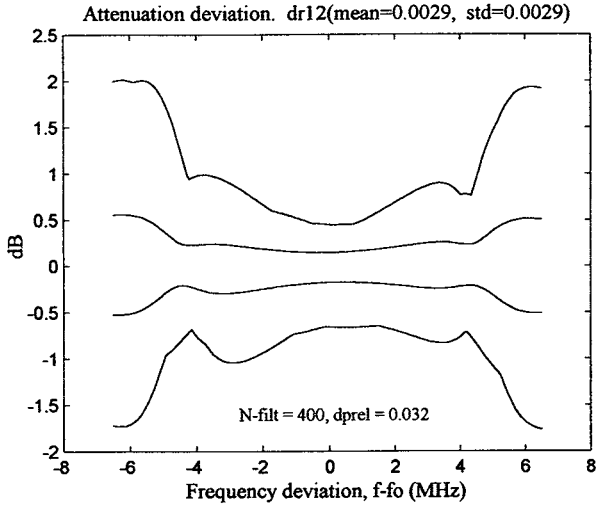

Figure 9. Attenuation deviation mask for filter shown in Figure 7. Outer lines: all filters. Inner lines: 2/3 of the filters comprised.

observe, although the zero/pole error tolerance becomes stricter as we go from Butterworth (0.025) to Tchebycheff and to Cauer (0.015).

For reasons that concern correlator performance it could be interesting to use narrower filters, e.g., 10 MHz bandwidth, with the same filter mask as before (Figures 7 and 8). In this case, the following conclusions can be drawn: (1) The required Butterworth filter order is reduced from 8 to 5, and the Cauer one is reduced from 7 to 5 or 4 (see conclusion 2) with the consequent filter fabrication and adjustment simplification. (2) The critical mask corner is now that going from -80 to -100 dB. If this could be relaxed, a fourth-order Butterworth or Cauer filter would also meet the specifications. (3) With regard to the inner mask it can now be clearly seen how the Butterworth one is wider (Figures 5 and 9), and it is also wider than the one corresponding to Cauer filters (Figures 9 and 10). This may indicate a better tolerance to the Butterworth filter's attenuation deviation, and since, on the other hand, their fabrication and adjustment are also less critical than in the other

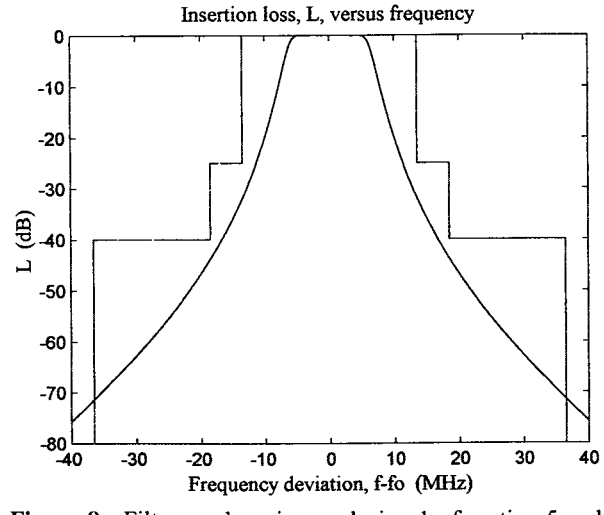

Figure 8. Filter mask as in conclusion 1 of section 5 and frequency response of a fourth-order, 10 MHz, 0.043 dB ripple elliptic filter.

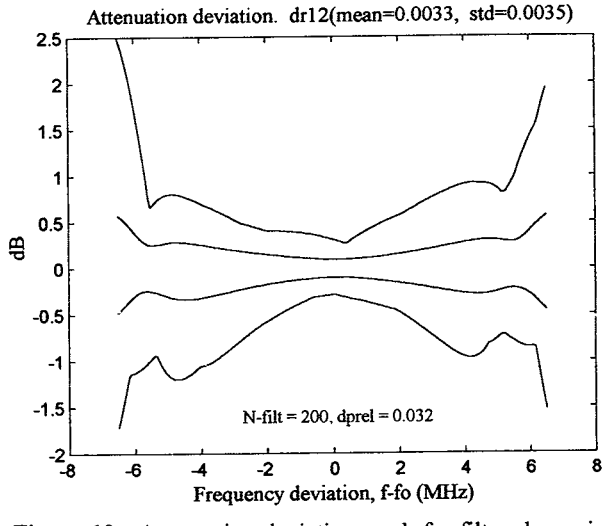

Figure 10. Attenuation deviation mask for filter shown in Figure 9. Outer lines: all filters. Inner lines: 2/3 of the filters comprised.

filter types, this filter is probably the best choice for MIRAS.

6. Conclusions

It has been shown that because of the powerful mathematical properties of the filters' transfer functions (analytic signals in the frequency domain) the requirements on the nonseparable phase errors and amplitude errors produced by deviations of the filters from their ideal model can be translated into requirements on the attenuation deviations only. It has also been proved that the effects of filter errors on the fringe-washing function amplitude error (fixed in previous studies, for in-orbit distributed noise injection calibration, as 0.3% for the tight 1 K sensitivity requirement) are more severe than on the phase ones.

For the filter specifications given in Conclusion 1, section 5, for MIRAS, these requirements are (1) that the rms attenuation deviation defined in the interval $(-1.3f_c, 1.3f_c)$, f_c being the ideal low-pass prototype cutoff frequency, does not exceed an average value 0.4 dB with a standard deviation of 0.16 dB or less and (2) alternatively, that every filter attenuation deviation lies between the outer lines of the corresponding masks in Figures 5, 6, and 9 and that two thirds of them lie between the inner ones.

Appendix A: Amplitude and Phase Relationships

1. Relationships between the deviation attenuation A_k and deviation phase Φ_k as defined by equations (5) and (6) are considered. Let $a_k(\tau)$ be the inverse Fourier transform of the deviation attenuation $A_k(f)$:

$$a_k(\tau) = \int_{-\infty}^{\infty} A_k(f) e^{j2\pi f\tau} df = \mathrm{F}^{-1}[A_k(f)]. \qquad \text{(A1)}$$

Then, (1)

$$\phi_k(\tau) = \mathrm{F}^{-1}[\Phi_k(f)] = j\,\mathrm{sgn}(\tau)\, a_k(\tau), \qquad \text{(A2)}$$

with the sign function, sgn (τ), defined such that sgn (0) = 0. (2) Hermitian property: $a_k(-\tau) = a_k^*(\tau)$. (3) If $A_k(f)$ is an even function, $\Phi_k(f)$ is odd, and vice versa. It can also be shown that:

$$\mathrm{A}_k(f) = 2\int_0^{\infty} a_k(\tau) e^{-j2\pi\tau} d\tau, \quad \int_{-\infty}^{\infty} \Phi_k(f) df$$

$$= j\,\mathrm{sgn}(0)\, a_k(0) = 0,$$

$$\int_{-\infty}^{\infty} A_k(f) df = -j\,\mathrm{sgn}(0)\,\Phi_k(0) = 0, \quad \int_{-\infty}^{\infty} A_k(f)\,\Phi_k(f) df$$

$$= j\int_{-\infty}^{\infty} \mathrm{sgn}(\tau)\,|a(\tau)|^2 d\tau = 0,$$

$$\|A_k\|^2 \quad \int_{-\infty}^{\infty} A_k^2(f) df = \|\Phi_k\|^2, \; \|\mathbf{A}_k\|^2 = 2\|A_k\|^2. \qquad \text{(A3)}$$

2. As for filter response frequency shifts, the deviation function $D_k(f)$ defined by (5), (6), and (8) is evidently useful for frequencies within the passband, but when the actual filter response is the ideal response shifted in frequency, the deviation attenuation $A_k(f)$ will tend to become very large as one approaches and trespasses the ideal filter cutoff frequencies. It is easy to see, for instance, that in the case of a theoretical rectangular ideal filter response, a frequency shift or bandwidth change results in infinite values for $A_k(f)$ in the frequency margin between the old and new (shifted) cutoff frequencies. In spite of this, it has been found that for the filters required for an actual radiometer like MIRAS these situations do not bring the values of the deviation attenuation beyond the limits permitted by the approximations used in the theoretical developments.

3. One point that deserves additional discussion is the hypothesis $A_k(\infty) = 0$, which amounts to a proper choice of attenuation reference level for each deviation function. In experimental work, with an upper frequency limit, this condition cannot be checked. In practice, if we are able to measure in a frequency range $(f_{\min}, f_{\max})$, we can approximately require that

$$\int_{-f_{\min}}^{f_{\max}} A_k(f) = 0, \qquad \text{(A4)}$$

which is a weak version of the corresponding equation (A3). Note that this condition is actually a definition of the zero level for the attenuation deviation.

Appendix B: Evaluation of the Phase of S_{12}

Let us consider the complex number z given by

$$z = A + \sum_{i=1}^{N} B_i \qquad A \geq \sum_{i=1}^{N} |B_i|. \qquad \text{(B1)}$$

Its phase can be computed by taking the imaginary part of its logarithm:

$$\ln z = \ln A + \ln\left(1 + \sum_{i=1}^{N} x_i\right) = \ln A + \sum x_i - \frac{1}{2}\left(\sum x_i\right)^2$$

$$+\frac{1}{3}\left(\sum x_i\right)^3 + \cdots = \ln A + \sum x_i - \frac{1}{2}\sum x_i^2 - \sum_i \sum_{j\neq i} x_i x_j$$

$$+\frac{1}{3}\sum x_i^3 + \cdots + G(B_1^p B_2^q, \ldots, B_N^t) = \ln A + \sum_{i=1}^{N} \ln(1 + x_i)$$

$$-\sum_i \sum_{j\neq i} x_i x_j + G(B_1^p B_2^q, \ldots, B_n^t)$$

$$x_i = B_i / A \qquad p + q + \cdots + t \geq 3 \qquad \text{(B2)}$$

Therefore, if A is assumed to be real,

$$\arg(z) = \sum_{i=1}^{N} \arg(A + B_i) - \mathrm{Im} \sum_{i} \sum_{i \neq j} \frac{B_i}{A} \frac{B_j}{A} + \arg(O \geq 3) \tag{B3}$$

where O is the order. Note that the separable terms are of first order on B_i while the nonseparable part has terms of second and higher order. Application of this equality to the expression of S_{12} given by (15) results, neglecting terms of third order or higher, in (17).

Appendix C: Evaluation of Upper Bounds for Small Deviations

This appendix is concerned with the evaluation of an upper bound for the magnitude defined by (18) in the main text. Since

$$\mathbf{A}_1^*(f) = 2\int_0^{\infty} a_1(-\tau) e^{j2\pi f\tau} d\tau = 2\int_{-\infty}^{0} a_1(\tau) e^{-j2\pi f\tau} d\tau,$$

$$\mathbf{A}_2(f) = 2\int_0^{\infty} a_2(\tau) e^{-j2\pi f\tau} d\tau,$$

$$\mathbf{A}_1^*(f) + \mathbf{A}_2(f) \quad \mathbf{A}_{12}(f) = 2\int_{-\infty}^{\infty} a_{12}(\tau) e^{-j2\pi f\tau} d\tau$$

$$a_{12}(\tau) \quad a_1(\tau)u(-\tau) + a_2(\tau)u(\tau) \tag{C1}$$

In the last equation $u(\tau)$ stands for the step function. The norm of $\mathbf{A}_{12}(f)$ can be computed as follows:

$$\|\mathbf{A}_{12}(f)\|^2 = \int_{-\infty}^{\infty} |\mathbf{A}_{12}(f)|^2 df = 4\int_{-\infty}^{\infty} |a_{12}(\tau)|^2 d\tau$$

$$= 4\int_{-\infty}^{0} |a_1(\tau)|^2 d\tau + 4\int_{0}^{\infty} |a_2(\tau)|^2 d\tau. \tag{C2}$$

Then, if the norms of the attenuation deviations are bounded $\|A_k(f)\| \leq N_A \rightarrow \|\mathbf{A}_{12}(f)\| \leq 2N_A$, (18) can be found:

$$\Delta S_{12}(\tau) = -\int_{-\infty}^{\infty} T(f)\mathbf{A}_{12}(f) e^{2j\pi f\tau} df \Rightarrow \|\Delta S_{12}(f)\|^2$$

$$\leq \|\mathbf{A}_{12}(f)\|^2 \int_{-\infty}^{\infty} T^2(f) df \leq 4N_A^2 B', \tag{C3}$$

with B' given by equation (D2). However, since $T(f)$ tends rapidly to zero outside its nominal passband ($-f_c$, f_c), the infinite range of integration can be replaced by ($-f_M$, f_M), with $f_M = \gamma f_c$, $1.2 < \gamma < 1.3$ (see appendix D). That is,

$$\Delta S_{12}(\tau) \approx \int_{-f_M}^{f_M} T(f)\mathbf{A}_{12}(f) e^{2j\pi f\tau} df,$$

$$\|\Delta S_{12}(\tau)\|^2 \leq B' \int_{-f_M}^{f_M} |\mathbf{A}_{12}(f)|^2 df. \tag{C4}$$

In order to find a suitable upper bound to the last integral a bound for the rms value of the attenuation deviation of each filter in ($-f_M$, f_M), $\sigma_{A1,2}$, in nepers, is introduced:

$$\int_{-f_M}^{f_M} |\mathbf{A}_{12}(f)|^2 df = B_M \sigma_{A1,2}^2 \leq B_M \sigma_A^2,$$

$$\int_{-f_M}^{f_M} |\mathbf{A}_{12}|^2 df \leq 4\alpha B_M \sigma_A^2 \quad B_M = 2f_M, \tag{C5}$$

where α is an unknown constant; however, since when $f_M \rightarrow \infty$, $\alpha \rightarrow 1$, it is expected that α be close to unity. Taking into account that $B' \approx 0.92B$, $B_M \approx 1.3B$ (appendix D), it can finally be written:

$$|\Delta S_{12}(\tau)| \leq 2\sqrt{\alpha B' B_M}\,\sigma_A \approx 2.2\sqrt{\alpha} B \sigma_A. \tag{C6}$$

Appendix D: Estimation of Bandwidths and Deviation Attenuation

An estimation of the bandwidths B' and B_M appearing in the analysis can be performed in the analytically simple case of an nth-order Butterworth band-pass filter:

$$H_o^2(f) = T(f) = \frac{1}{1 + (f/f_c)^{2n}}. \tag{D1}$$

It has been shown that the order required for MIRAS is $n \geq 5$. If we take $n = 5$, it can be computed that:

$$B = \int_{-\infty}^{\infty} T(f) df = 1.02(2f_c), \quad B' = \int_{-\infty}^{\infty} T^2(f) df = 0.91B,$$

$$\int_{-f_M}^{f_M} T(f) df = r \int_{-\infty}^{\infty} T(f) df \quad r_{(\gamma=1.2)} = 0.98; \; r_{(\gamma=1.3)} = 0.99. \tag{D2}$$

Of course, both B' and $2f_M$ approach $2f_c$ as n increases, since, when $n \rightarrow \infty$, the filter approaches an ideal rectangular function. From (C2) it can be seen that if the actual filter cutoff frequencies f_{c1} and f_{c2} are restricted to deviate from the ideal ones ($-f_c$, f_c) by not more than 10% (0.10), then for any two filters labeled 1 and 2,

$$\left(\int_{-\infty}^{-1.3f_c} + \int_{1.3f_c}^{\infty} \right) |H_{o1}(f) H_{o2}^*(f)| df$$

$$\leq \left(\int_{-\infty}^{-1.2f_c} + \int_{1.2f_c}^{\infty} \right) |H_{o1}(f) H_{o2}^*(f)| df$$

$$\approx \left(\int_{-\infty}^{-1.2f_c} + \int_{1.2f_c}^{\infty} \right) |H_o(f)|^2 df = 0.02B \tag{D3}$$

and replacement of the infinite limits by the finite limits ($-1.3f_c$, $1.3f_c$) produces a relative error of less than 2%.

This filter response can also be used to estimate the values of the deviation attenuation $A_k(f)$ in case of a frequency shift, mentioned in appendix A. For fifth- and seventh-order Butterworth filters, a 5% shift, which for a bandwidth of 20 MHz (as in MIRAS) results in an absolute deviation of 1.0 MHz, the peak value of $A_k(f)$ increases with the filter order but remains below 0.27 Np = 2.34 dB. It also turns out that the rms attenuation deviation (computed with $f_M = 1.3f_c$) is $\sigma_A = 0.75$ dB for $n = 5$ and $\sigma_A = 1.10$ dB for $n = 7$. Therefore it can be said that for the requirements of a radiometric interferometer like MIRAS the formulation of the problem in terms of the deviation function $D_k(f)$ is adequate.

Appendix E: Evaluation of the Amplitude Error (Equation (26))

Since

$$\ln(z) = \ln\left(|z|e^{j\psi}\right) = \ln|z| + j\psi, \qquad \text{(E1)}$$

examination of (B2) leads, to second-order approximation, to

$$\ln|z| = \mathrm{Re}(\ln z) = \ln A + \mathrm{Re}\left[\sum_{i=1}^{N} \ln\left(1+\frac{B_i}{A}\right) - \sum_i \sum_{j\neq i} \frac{B_i}{A}\frac{B_j}{A}\right]. \qquad \text{(E2)}$$

To arrive at (26), it has just to be considered, together with (E2), that

$$\ln(\tilde{r}_{12}) = \ln(S_{12}) - \frac{1}{2}\ln(S_{11}) - \frac{1}{2}\ln(S_{22}),$$
$$S_{12} = S + \Delta S_1 + \Delta S_2 + \Delta S_{12}^{(2)},\ S_{11} = S + 2\Delta S_1 + \Delta S_{11}^{(2)}$$
$$S_{22} = S + 2\Delta S_2 + \Delta S_{22}^{(2)}. \qquad \text{(E3)}$$

From these equations we obtain

$$\ln|\tilde{r}_{12}| = \ln(1+\Delta|\tilde{r}_{12}|) \approx \Delta|\tilde{r}_{12}| \approx \frac{1}{2S}\mathrm{Re}(2\Delta S_{12}^{(2)} - \Delta S_{11}^{(2)} - \Delta S_{22}^{(2)}) + \frac{1}{2S^2}\mathrm{Re}(\Delta S_1 - \Delta S_2)^2, \qquad \text{(E4)}$$

and (26) immediately follows.

Acknowledgments. This work has been supported by the Spanish Research Project CICYT TIC 96/0879 and also partly by the European Space Agency on its development of MIRAS-LICEF (Light & Cost Effective Front-End) and MIRAS Calibration System Definition (CAS-D) activities (ESTEC contract 12513/97/NL/MV).

References

Camps, A., F. Torres, J. Bará, I. Corbella, and F. Monzón, Automatic calibration of channels frequency response in interferometric radiometers, *Electron. Lett.*, *35*(2), 115-116, 1999.

Martín-Neira, M., and J.M. Goutoule, MIRAS: A two-dimensional aperture-synthesis radiometer for soil-moisture and ocean salinity observations, *ESA Bull.*, *92*, 95-104, 1997.

Thomson, A.R., J.M. Moran, and G.W. Swenson, *Interferometry and Synthesis in Radio Astronomy*, John Wiley, New York, 1986.

Torres, F., A. Camps, J. Bará, I. Corbella, and R. Ferrero, On-board phase and module calibration of large aperture synthesis radiometers: Study applied to MIRAS, *IEEE Trans. Geosci. Remote Sens.*, *34*(4), 1000-1009, 1996.

Torres, F., A. Camps, J. Bará, and I. Corbella, Impact of receiver errors on the radiometric resolution of large two-dimensional aperture synthesis radiometers, *Radio Sci.*, *32*(2), 629-641, 1997.

Van Valkenburg , M.E. *Network Analysis*, Prentice-Hall, Englewood Cliffs, N. J., 1955.

J. Bará, A. Camps, I. Corbella, and F. Torres, Polytechnic University of Catalonia, Campus Nord, D3, c/ Jordi Girona 1-3, 08034 Barcelona, Spain. (bara@tsc.upc.es; camps@tsc.upc.es; corbella@tsc.upc.es xtorres@tsc.upc.es;)

(Received December 8, 1998; revised March 27, 2000; acccepted April 18, 2000.)